Industrial Crops & Products 151 (2020) 112475

Contents lists available at ScienceDirect

Industrial Crops & Products

journal homepage: www.elsevier.com/locate/indcrop

Enhanced hydrophobicity of soybean protein isolate by low-pH shifting treatment for the sub-micron gel particles preparation

Yufei Yang[a], Shudong He[a,*], Yongkang Ye[a], Xiaodong Cao[a], Haiyan Liu[b,c], Zeyu Wu[a], Junyang Yue[a], Hanju Sun[a]

[a] School of Food and Biological Engineering, Engineering Research Center of Bio-process of Ministry of Education, Hefei University of Technology, Hefei 230009, Anhui, PR China
[b] Sichuan Huamei Pharmaceutical Co., Ltd., Chengdu Sanojon Pharmaceutical Group, Chengdu 610045, Sichuan, PR China
[c] Dairy Nutrition and Function, Key Laboratory of Sichuan Province, Chengdu 610000, Sichuan, PR China

ARTICLE INFO

Keywords:
Soybean protein isolate (SPI)
Low-pH shifting treatment
Functionality
Soluble soybean polysaccharide (SSPS)
Maillard reaction
Sub-micron gel particles

ABSTRACT

In the present study, the soybean protein isolate (SPI) was treated by pH shifting process, as the protein was incubated in low pH solutions (pH 1.5–3.5) for 12 h, following neutralized to pH 7.0 and held for 4 h, which resulted in a conformation unfolding/refolding confirmed by the fluorescence spectra and a substantial increase in α-helix content revealed by circular dichroism (CD) spectra, along with the increased exposure of hydrophobic and sulfhydryl groups. In addition, the heat-induced gelation process and enhanced gel strength of pH 3.0 and 3.5 shifted SPIs were observed. Maillard reaction was then applied and the glycosylated SPI was further applied to the sub-micron gel particles formation. Results showed that low-pH shifting obviously improve the glycosylation ability of SPI as the conjugation degree and browning degree were enhanced. The sub-micron gel particles with core–shell structure and the average sizes of 100–250 nm were formed via heating self-assembly reaction and confirmed through Z-average of particle size, meanwhile, the increasing stability of gel particles in the solution was determined by Zeta potential analysis, suggesting that the improvement of hydrophobicity and glycosylated ability of SPI could promote gelling properties. Hence, the protein modification stage of pH shifting process would provide a great potential application in the formation of nano- or microscale gel particles.

1. Introduction

With increasing application of the nano- and microscale biopolymer particles in drug delivery and bioactive compounds encapsulation, the development of green and environment-friendly preparation processes has attracted researchers (Britto et al., 2014; Champagne and Fustier, 2007; Li et al., 2008; Przybyla and Chmielewski, 2010). Although synthesized polymers or blending with natural materials have been widely applied in the nanogel particles formation because of the advantages in environmental response, tunable drug loading and release properties (Wang et al., 2010), the organic solvent requirement and worse biocompatibility *in vivo* of most synthesized polymers lead to the exploration of pure proteins/polysaccharides in this area.

It has been well known that many natural proteins/polysaccharides, such as soy protein, whey protein, albumin, casein (Bar-Zeev et al., 2016; Sáizabajo et al., 2013), silk fibroin (Lammel et al., 2010) and cellulose (Zhu et al., 2013), have the unique amphiphilic and self-assembling abilities, and could built the biocompatible gels with non-covalent bonds, such as hydrogen bond, electrostatic attraction, and disulfide bond. It is noteworthy that soybean protein and soluble soybean polysaccharide (SSPS) have been widely used in the preparations of embedding and delivering particles and/or emulsions (Fernandez-Avila et al., 2016). As one of the easily obtained and low-cost vegetable protein source, soybean protein isolate (SPI) composed of glycinin (11S) and β-conglycinin (7S), and SSPS containing anionic polysaccharides with pectin-like structure could be extracted from the by-product of SPI (Tu and Rousseau, 2013). In a certain concentration of SPI and SSPS mixture, when the environmental pH value was lower than the isoelectric point (IEP) of SPI, the cations on the surface of SPI would link to the anions of galacturonic acid in SSPS, thereby providing the probability in nanomaterial preparation. The core–shell particles performed as carriers for curcumin were prepared, and Zeta potential analysis proved that SSPS was bound to surface of highly aggregated SPI core after adjusting solution pH from 7.0 to 4.0 (Chen et al., 2016). In addition, in view of the importance of size control, the materials as well as methods of nanoparticle preparation should be further

* Corresponding author.
E-mail address: shudong.he@hfut.edu.cn (S. He).

https://doi.org/10.1016/j.indcrop.2020.112475
Received 9 December 2019; Received in revised form 9 April 2020; Accepted 11 April 2020
Available online 27 April 2020

researched. Ding and Yao (2013) have produced the nanogels of SPI and SPSS via high-pressure homogenization and acidic solution environment to prevent the original aggregates of soy protein, and the D_h (Z-average hydrodynamic diameter) of nanogels were about 100–200 nm in final. But, the applications of hydrophobic and electrostatic forces to control the particle size and stability of soy protein/polysaccharide nano-gels have not been well-documented yet.

According to the previous studies, the nanospheres or sub-microspheres (diameter range of 1–1000 nm) on pharmaceutical preparations would be superior to micron particles in the light of stable dispersion (Sun et al., 2010), non-toxicity, and crossing biological barriers (Rabanel et al., 2012). Then, in order to reach the sub-micron scale, a vital bottom-up strategy by using the self-assembly (Biswas et al., 2012) was applied in the preparation of natural materials, where glycosylation and heat-induced gelation would play auxiliary roles in the formation of protein-polysaccharide conjugates and stable gel particles. The nanogels with a lysozyme core and dextran shell have been developed via Maillard dry-heat process and heat-gelation process (Li et al., 2008), and the nanoparticles of bovine serum albumin (BSA)-dextran encapsulated with the ibuprofen were also achieved by this strategy (Li and Yao, 2009). However, the formation of stable soy protein gel without cross-linking agents must rely on the intermolecular forces (Batista et al., 2005), then the hydrophobicity might be of importance to ultimately control the size, shape and even loading capacity of the gel particles in a certain degree. Outstanding solubility (Puppo et al., 2004), rheological properties (Speroni et al., 2009), and stability (Manassero et al., 2015) characteristics of SPI were obtained by heating and high-pressure (Liu and Zhao, 2010; Molina and Ledward, 2003) via structural modification owing to the protein unfolding and exposure of hydrophobic groups. However, the industrial applications would be limited because of the high requirements of equipment and energy consumption. Then as a chemical modification realized by strong acid-base regulation, pH shifting proposal might open a new avenue for easier protein conformational changes. By exposing the protein to extreme pH incubation followed by neutralization, a loose of conformational state between the secondary and tertiary structures was obtained (Jiang et al., 2012). According to the previous studies, the gelling property of SPI was availably improved via a combination of pH 1.5 shifting and mild heating processes (Liu et al., 2015), furthermore, the exposure of hydrophobic group of SPI was conferred by the extreme low-pH (pH 1.5) treatments (Jiang et al., 2012; Jiang and Xiong, 2013). With the improvement of solubility, hydrophobicity and emulsifying properties via extreme pH treatment, the pH shifting SPI was used in film formation (Jiang et al., 2012) and the structure-reinforcement of pork myofibrillar gels (Jiang and Xiong, 2013). However, the gel particles produced by low-pH shifting proteins have not been reported, and moreover, the micro-control research on SPI functionality in low pH range was insufficient as well.

In the present work, the structural alterations of low-pH shifting SPI were investigated by intrinsic/extrinsic fluorescence spectra, sulfhydryl content and circular dichroism (CD) spectra, respectively, and gelling properties were determined by rheological study. Furthermore, the SPI-SSPS conjugates were characterized by FTIR spectroscopy, conjugation degree, and browning degree. The particle size distribution and stability of gel particles prepared by self-assembly in solution were evaluated by scanning electron microscopy (SEM), transmission electron microscopy (TEM) and Zeta potential analysis. The crucial hydrophobicity established by the structural modification of SPI was investigated in controlling self-assembly process, and the results would be beneficial to the gel particle preparation.

2. Materials and methods

2.1. Materials

Soy protein isolate (SPI, Purity > 90 %) was purchased from Shansong Biological Products Co., Ltd. (Linyi, Shandong province, China). Soluble soybean polysaccharide (SSPS, Effective substance content 99 %) was obtained from Jinjing Biotechnology Co., Ltd. (Pingdingshan, Henan province, China). All chemicals and solvents were of analytical grade.

2.2. Sample preparation

2.2.1. Low- pH shifting treatment of SPI

SPI powders were suspended in distilled water to obtain a concentration of 30 mg/mL, and then stirred with a magnet bar for 30 min to obtain a uniform dispersion. After the centrifugation at 10,000 g for 15 min at 4 °C, the supernatant was diluted to the concentration of 20 mg/mL. Then the protein solution was adjusted to low pH values (1.5, 2.0, 2.5, 3.0, and 3.5, respectively) by using 2 M HCl and was incubated for 12 h at room temperature (25 ± 2 °C). Finally, the protein dispersions were neutralized to pH 7.0 and held for 4 h. The SPI without pH shifting was set as control by pH adjustment to pH 7.0. All samples were dialyzed for 48 h at 4 °C, then lyophilized and stored in -80 °C for further analysis.

2.2.2. SPI-SSPS conjugate preparation

SPIs and SSPS (1:1, w/w) were dispersed in deionized water with final concentrations of 1% (w/w), respectively. The sample solutions were stirred at room temperature for 2 h and stood at 4 °C for 12 h to ensure the complete hydration. Each sample was placed in a water bath heated at 95 °C for 6 h, and then centrifuged at 7195 g for 30 min. SPI-SSPS conjugate powders were obtained after freeze-dried.

2.2.3. Gel particle preparation

SPI-SSPS conjugate powders were prepared with deionized water and dissolved in 1 mg/mL by stirring for 30 min. The pH values of the solutions were adjusted to 3.8, 4.0, 4.2, 4.4, and 4.6 with 0.1 M HCl, respectively, then balanced for 5 min. After incubation in water bath at 90 °C for 60 min, the SPI-SSPS gel particle solution was obtained in final.

2.3. Intrinsic and extrinsic fluorescence analysis

In the intrinsic analysis, the samples were dispersed in a phosphate buffer (0.01 M, pH 7.0) and diluted to the final concentration of 1 mg/mL. The emission spectra of 300–400 nm with slit width of 5 nm and scanning speed of 300 nm/min were obtained by using a F97pro fluorescence spectrophotometer (Lengguang Tech., Shanghai, China) at the excitation wavelength of 295 nm and slit width of 5 nm. The pure phosphate buffer was regarded as blank.

The surface hydrophobicity was determined by the extrinsic fluorescence analysis referring to the method of Liu et al. (2015). The protein solution of 20 mg/mL was prepared by using a phosphate buffer (0.01 M, pH 7.0) and diluted in the range of 0.005–0.50 mg/mL. Fifty microliters of ANS (8 mM) prepared in a phosphate buffer (0.01 M, pH 7.0) was added into each sample of 4 mL. The fluorescence intensity of proteins was measured at excitation wavelength of 394 nm and emission wavelength of 483 nm, respectively. The surface hydrophobicity index (S_0) was shown by the initial slope of fluorescence intensity and protein concentration.

2.4. Circular dichroism (CD) spectra analysis

The influence of pH shifting on the secondary structure of SPIs was analysed by using a Chirascan CD spectrometer (Applied Photophysics Ltd., UK). Each sample (0.5 mg/mL) was dissolved in 10 mM phosphate buffer at pH 7.0 and scanned 5 times at 25 °C in the region of 190–250 nm. The CD signals were recorded under 1.0 nm bandwidth, 0.2 nm step resolution, and 100 nm/min scan rate. The pure phosphate buffer was used as blank.

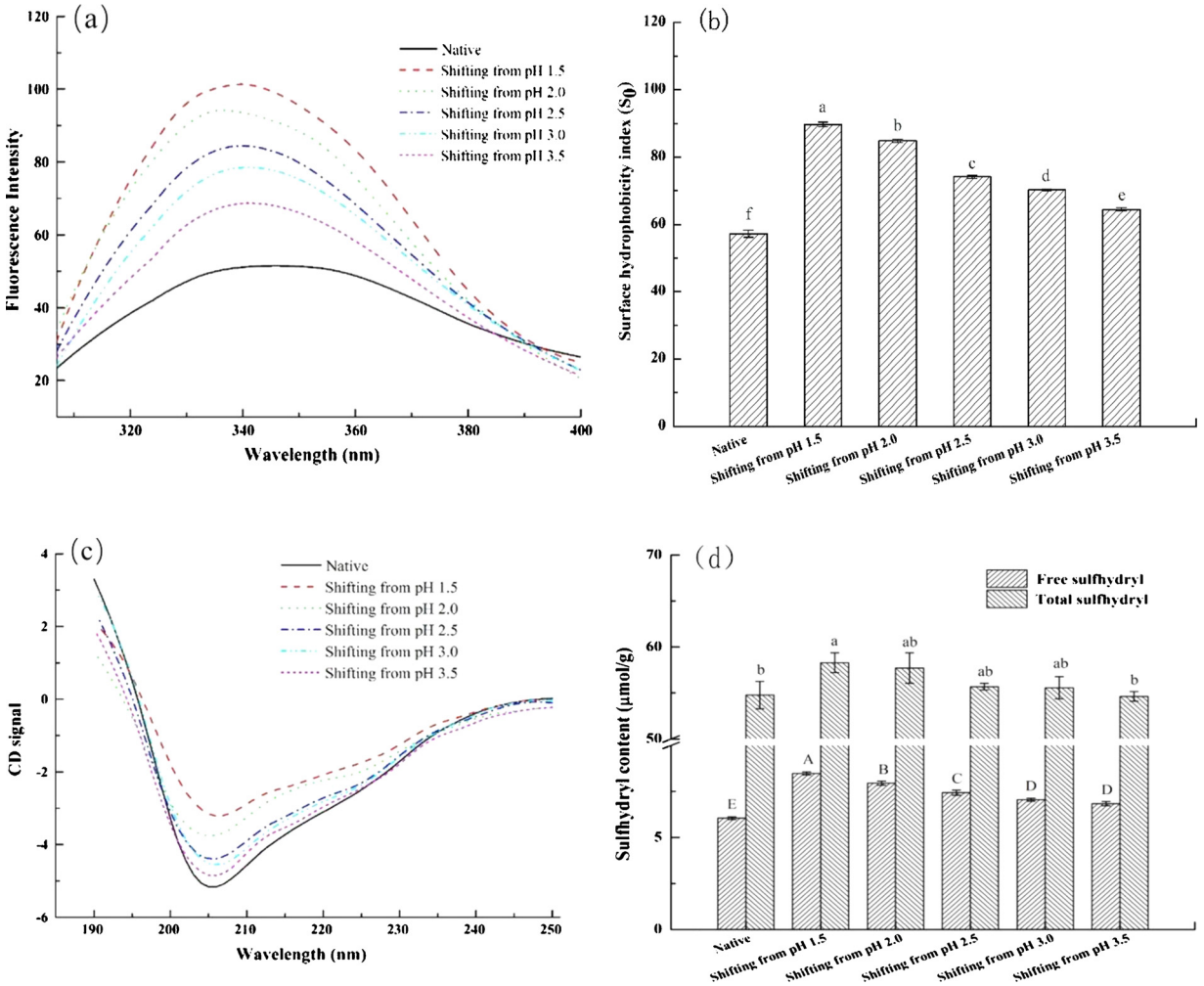

Fig. 1. Structural analysis of the low-pH shifted SPIs. (a) Intrinsic fluorescence spectra of the native SPI and the SPIs shifting from pH 1.5, 2.0, 2.5, 3.0, and 3.5. (b) Surface hydrophobicity index (S_0), error bars denote standard error (SD, n = 3) and different lowercase letters indicate significant differences ($P < 0.05$) between each sample. (c) Far ultraviolet circular dichroism spectra of SPIs swept at the wavelength from 190 to 250 nm. (d) Sulfhydryl content of the native and pH shifting SPIs, respectively. Error bars denote standard error (SD, n = 3). Different capital letters mean significant differences ($P < 0.05$) among free sulfhydryl of different SPI groups, while different lowercase letters mean significant differences ($P < 0.05$) among total sulfhydryl groups.

2.5. Sulfhydryl and disulfide contents determination

SPI samples (50 mg) were suspended in 10 mL phosphate buffer (0.1 M, pH 8.0, containing 1% sodium dodecyl sulphate and 1 mM EDTA) by occasional vibrating for 1 h and then centrifuged for 15 min at 10,000 g. Bovine serum albumin (BSA) was used as the standard to determine the soy protein concentration in the supernatant. Sulfhydryl (free SH) and total sulfhydryl (SH and reduced SS) contents were measured based on Ellman's reagent colorimetric method described by Huang et al. (2006). The absorbance of the supernatant was read at 412 nm with the reagent buffer as blank, and SH contents were calculated using the extinction coefficient of 13,600 $M^{-1}cm^{-1}$ (Ellman, 1959).

2.6. Gelling properties determination

The gelling properties of SPI were characterized by dynamic measurements with a rotational rheometer (Discovery DHR-3, TA, USA) fitted with parallel plates (40 mm diameter and 1 mm gap). Measurements were performed at a constant strain of 0.02 %, which was within the linear region, and at an angular frequency of 1 Hz. To induce gel formation, samples were heated from 25 to 95 °C at a heating rate of 2 °C/min, kept at 95 °C for 15 min, and cooled down to 25 °C at a cooling rate of 4 °C /min. During the experiment, a two-piece cover was applied to avoid the water evaporation. The storage modulus (G'), loss modulus (G") and loss tangent (tan δ) of each sample were recorded.

2.7. Fourier transform infrared (FTIR) spectra analysis

The freeze–dried powders of SPI-SPSS conjugate (2 mg) were mixed with potassium bromide (100 mg) and made into pellets, respectively. The absorbance was measured in the range of 4000–400 cm^{-1} during 32 scans with 4 cm^{-1} resolution by a Nicolet 67 FTIR spectrometer (Thermo Nicolet Co., USA) and analysed by means of Peak Fit 4.12 (Systat Software, San Jose, CA).

2.8. Conjugation and browning degree determination

The free amino groups content of protein was determined and the conjugation degree was obtained referring to Penas et al. (2004).

The browning degree of SPI-SSPS was characterized with the spectrophotometry at 294 and 420 nm, and the glycosylated ability was compared through the absorbance.

2.9. Morphology analysis

The morphology of the samples was observed by a 120 kV transmission electron microscopy (TEM, Tecnai G2 Spirit BioTWIN, FEI, OR, USA) and a scanning electron microscopy (SEM, JSM-6490LV, JEOL, Japan), respectively. Prior to the TEM survey, the gel particle solutions were dropped onto the copper net coated with carbon film, and then dried after being dyed with uranyl acetate. In the SEM observation, the gel particle solutions were dried and coated with gold.

2.10. Particle size distribution and zeta potential determination

The particle size distribution and Zeta potential were measured by a Nano-ZS90 Zeta potentiometer (Malvern Co., UK). Water was chosen as the dispersant with viscosity of 0.8872 cP and dispersant refractive index (RI) was set as 1.330. The concentration of each gel particle sample was adjusted to 1 mg/mL, and as comparisons, pH shifting SPIs were also dissolved in water with the same pH and concentration of 1 mg/mL (w/v). The Z-average (mean hydrodynamic diameter) of particle size and Zeta potential were obtained at room temperature (25 ± 0.1 °C) after equilibrium time of 120 s.

2.11. Statistical analysis

All measurements were carried out in triplicate unless otherwise stated. Values given in the tables and figures were the means of triplicates, and error bars indicated the standard deviation. Statistical significance of differences among means was evaluated by one-way analysis of variance (ANOVA) and Tukey test at 5% level of probability ($P < 0.05$).

3. Results and discussion

3.1. Low-pH shifting treatment improved the hydrophobicity of SPI

The protein hydrophobicity was reflected by the intrinsic and extrinsic fluorescence spectra (Fig. 1). Maximum absorption wavelength (λ_{max}) of the native SPI was 346 nm (Fig. 1(a)). With decreased pH values, the fluorescence intensity of each sample increased constantly, accompanied by a blue shifting of λ_{max} from 346 to 336 nm. The similar blue shifts of λ_{max} with the increases in fluorescence intensity were also found in pH 1.5 shifting SPI or extreme acidic pH shifting combined with mild heating treated SPI (Jiang et al., 2009; Liu et al., 2015), which might be attributed to the shift of the tryptophan microenvironment toward to a more hydrophobic environment (Liu et al., 2015). The surface hydrophobicity of SPI increased dramatically after low-pH shifting in Fig. 1(b). Surface hydrophobicity index (S_0) of SPI shifting from pH 1.5 (89.70 ± 0.71) was 1.57 folds than that of native SPI (57.26 ± 1.08). Obviously, the lower pH incubation resulted in a larger occurrence and exposure of hydrophobic regions of SPIs, reflecting an increase in S_0 and corresponding to the study of Jiang et al. (2012). Furthermore, these phenomena were contrasted to the samples treated by extreme alkaline pH shifting and simultaneously explained by more extensive unfolding resulting from intramolecular electrostatic repulsions (Jiang et al., 2011).

Effect of low-pH shifting on the secondary structure of SPI was observed by far ultraviolet CD spectroscopy (Fig. 1(c)). The curve of SPI displayed a minimum value near 208 nm, where the peak represents π–π* transition of α-helix (Sun et al., 2017). The negative CD signals of SPIs at 208 nm were significantly weakened when shifting pH from neutral, denoting the loss of α-helix structure (Liu et al., 2008). The changes of secondary structure inevitably led to the alterations of tertiary structure and suggested the structure of intermediate state between denaturation and non-denaturation of SPIs as well (Ptitsyn et al., 1990). In addition, a good negative correlation between α-helix content and surface hydrophobicity had also been observed by Kato et al. (1981) in the conformation of ovalbumin and lysozyme, respectively. Thus, with the decreases in helical content, intramolecular hydrophobic sites were exposed simultaneously, and the value of S_0 increased, which was in agreement with our fluorescence spectra analyses.

3.2. Sulfhydryl (SH) content of low-pH shifted SPI confirmed the increase of hydrophobicity

The sulfhydryl content of SPI after pH shifting was shown in Fig. 1(d). The trends of free SH content were similar to the total SH content, however, significant differences between the native and pH 1.5 shifting groups were observed in details (Fig. 1(d)). Specifically, the free SH contents of the native SPI (6.05 ± 0.08 μmol/g) was lower than the SPI shifting from pH 1.5 (8.49 ± 0.09 μmol/g), and the total content of sulfhydryl groups of pH 1.5 shifting SPI (58.29 ± 1.07 μmol/g) was higher than the native sample (54.77 ± 1.49 μmol/g). Changes of SH content might be resulted from the exposure of internal SH groups owing to protein unfolding during acidic treatment (Gu et al., 2009), or the cleavage of disulfide bonds (Hwang and Damodaran, 2015). Comparing to pH 1.5 group, the SPI shifting from pH 3.5 displayed a more limited denaturation because of acidic pH near isoelectric point of SPI (pH ~4.6). The increasing trends of SH content in pH shifting SPIs were relatively consistent with hydrophobicity analyses, which could be also explained by unfolding structure of proteins (Liu et al., 2015).

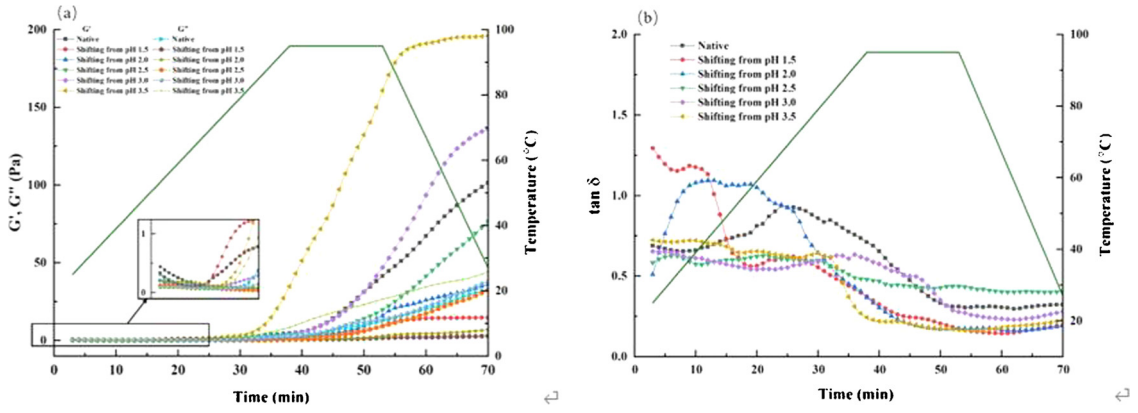

Fig. 2. Gelation process and gel strength of SPIs. (a) Changes of G' and G" in heating-cooling circle. (b) Loss tangent (tan δ) plots of SPIs. The native SPI, the SPIs shifting from pH 1.5, 2.0, 2.5, 3.0, and 3.5 shown with symbols in different colours and types.

3.3. Hydrophobicity enhanced gelling property of SPI

The gelling property of SPI (9 %, w/v) after low-pH shifting would be displayed by using the storage modulus (G'), loss modulus (G") and loss tangent (tan δ) (Fig. 2). The increased G' and G" as well as undulating plots of tan δ were found in each sample with the increases of both temperature and time, indicating various gelling abilities of SPIs. Generally, three stages would be undergone in the gelation of soybean protein: (1) protein denaturation and exposure of hydrophobic residues, (2) aggregation through intermolecular hydrophobic interaction of proteins, and (3) formation of network gel (Clark et al., 2001), and simultaneously, hydrophobic interactions and hydrogen bonds were identified as the major forces/bonds involving in gelation process (Paulson and Tung, 1989). Comparing to the native SPI, the increase of G' indicated the higher elasticity or gel strength in pH 3.0 and 3.5 samples, nevertheless, the G' of pH 1.5 shifted SPI was about 15 Pa in final. The improvement of hydrophobicity and sulfhydryl groups content could effectively enhance the gel strength of proteins in general, while the hydrophobic aggregation of protein would be accompanied with the decrease of solubility (Kristinsson and Hultin, 2004). When soy proteins were shifted from extreme acidic pH, insoluble aggregates even precipitates were generated and not incorporated owing to the enhanced hydrophobicity, providing fewer binding sites for cross-linking proteins into a network, and thereby leading to a lower gel strength (Renkema et al., 2002). The effect of pH shifting on SPI gelation was further demonstrated by heat-induced viscoelastic changes in protein solution according to tan δ. As shown in Fig. 2(b), different from the lower tan δ values in pH 2.5, 3.0 and 3.5 shifting SPIs, the G' and G" have dominated in pH 1.5 and 2.0 samples during different temperature periods, respectively. The protein solution of pH 1.5 shifting SPI had better viscosity (tan $\delta > 1$) in initial time and changed into elasticity dominance at 45 °C, while pH 2.0 sample was changed at 63 °C.

3.4. Structural features of SPI-SSPS conjugates via Maillard reaction

The structural analysis of glycosylated SPI was shown in Fig. 3 with the characteristic absorption peaks of SPI and SSPS. The secondary structure of SPIs based on amide I region was mainly resulted from C═O stretching vibration in the 1700–1600 cm^{-1}, where α-helix, β-sheet, β-turn, and random coils were located at 1650–1658, 1610–1640, 1660–1700, and 1640–1650 cm^{-1}, respectively (Wang et al., 2015). Furthermore, the contents of α-helix (Table 1) in pH shifting groups decreased comparing to the native, and showed a weakening trend with the pH reducing, which was in agreement with the qualitative results of the CD analysis. Since the carbohydrate region in the 1200–900 cm^{-1} and the "fingerprint" or anomeric region of carbohydrates in the 900–700 cm^{-1} were encompassed (Prado et al., 2005), the 1200–700 cm^{-1} spectral region was selected from IR spectra of SSPS for the further investigation (Fig. 3(a)). Typically, the specific peaks near 814 and 870 cm^{-1} were related with the presence of α-D-galactopyranose units and β-D-mannopyranose units, respectively (Buriti et al., 2014; Pawar and Lalitha, 2014), where the SSPS was demonstrated remaining its original structure even bonded with SPIs. The overall results suggested the formation of SPI-SSPS conjugates and an enhanced glycosylation ability of SPIs through low-pH shifting treatment.

3.5. Hydrophobicity improved conjugation degree of SPI and SSPS

A nonenzymatic reaction based on the Maillard reaction between carbonyl groups and amino groups could cause remarkable changes in structures and colours and thus conjugation degree was evaluated indirectly by the decreases of free amino acids (Nasrollahzadeh et al., 2017; Wang et al., 2017). Therefore, the enhanced grafting process of sugar molecules to protein has been confirmed by means of the increase of conjugation degree. As shown in Table 1, the noteworthy increasing trend was found in the degree of covalent conjugation of pH shifted SPIs. The group after extreme pH shifting expressed a greater glycosylation, and moreover, significant differences were observed comparing to that of native. The looser structure of protein molecules created by the low-pH treatment would result in an increased contact between the carbonyl and amino and thereby formed more protein-polysaccharide covalent conjugates and remained less free amino. In addition, the improved conjugation degree at low pH indicated that the increase of protein hydrophobicity was beneficial to glycosylation.

3.6. Browning degree of SPI-SSPS confirmed the benefits of hydrophobicity on glycosylation

The colourless intermediate compounds and browning pigments formed in the Maillard reaction process would be indicators according to the absorbance of 294 and 420 nm (Nooshkam and Madadlou, 2016), respectively. Therefore, the glycosylation degree of SPI was further characterized by the absorbance value of Maillard products (Table 1). As observed, absorbance values increased with low-pH treatment both in intermediate and final products, especially displayed in the pH 1.5 shifting group of which tertiary structure was partially unfolded, then carbonyl-amine reaction was intensified, and more intermediate and final compounds were produced. However, after a relatively high acidic pH treatment (pH 3.5), no increase in the absorbance at 294 nm but a slight increase at 420 nm were found compared with the native SPI. Thus, it seemed that low-pH shifting treatment would promote the glycosylation reaction of SPI and had more highlights in the extreme

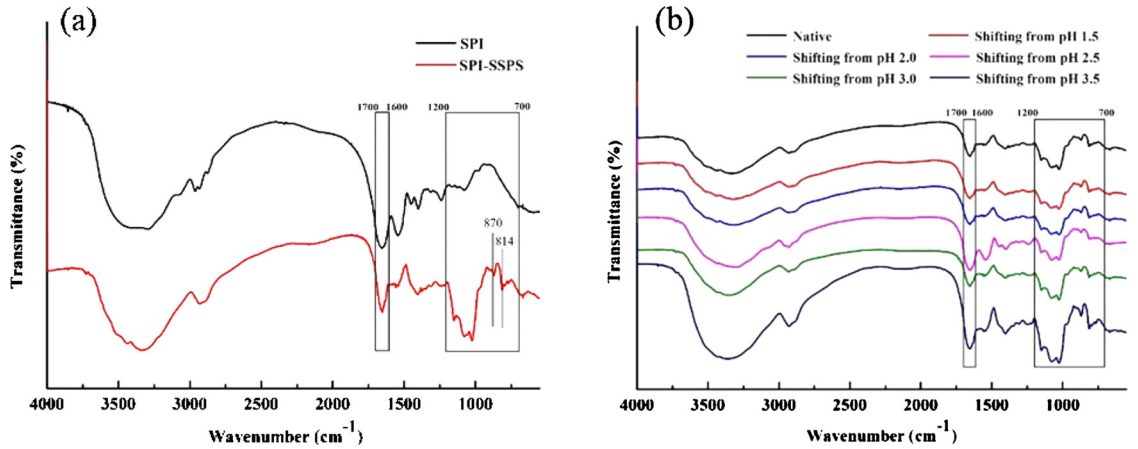

Fig. 3. The FTIR of SPI and SPI-SSPS after shifting from low-pH values. (a) Comparison of the native SPI and SPI-SSPI conjugate (b) The glycosylation of SPIs after different pH shifting.

Table 1
The content of α- helix, β-sheet, β-turn, and random coil in the range of amide I region, and the influence of SPI after low-pH shifting treatment on conjugation and browning degree.

SPI samples	Secondary structure content				Conjugation degree (%)	Browning degree	
	α-helix (%)	β-sheet (%)	β-turn (%)	random coil (%)		A_{294nm}	A_{420nm}
Native	22.86	14.41	46.17	15.95	63.56 ± 0.17^{e}	0.38 ± 0.00^{c}	0.19 ± 0.00^{d}
Shifting from pH 1.5	18.40	16.34	47.66	17.59	68.08 ± 0.02^{a}	0.44 ± 0.00^{a}	0.28 ± 0.01^{a}
Shifting from pH 2.0	18.67	13.75	51.82	15.28	65.91 ± 0.19^{b}	0.40 ± 0.00^{b}	0.24 ± 0.00^{b}
Shifting from pH 2.5	19.96	19.78	42.75	17.51	65.42 ± 0.05^{c}	0.40 ± 0.00^{b}	0.24 ± 0.00^{b}
Shifting from pH 3.0	20.80	18.19	45.31	15.69	65.09 ± 0.03^{c}	0.39 ± 0.00^{b}	0.23 ± 0.00^{b}
Shifting from pH 3.5	20.95	16.18	46.55	16.32	64.45 ± 0.16^{d}	0.38 ± 0.00^{c}	0.21 ± 0.01^{c}

Different lowercase letters indicate significant differences ($P < 0.05$) between each other in the same column.

acidic conditions.

3.7. pH condition selection for the gel particles incubation

Since the self-assembly of the SPI-SSPS conjugation was controlled by the environment pH and heating process for the protein denaturation, the range of incubated pH value was chosen from 3.8 to 4.6 considering two factors: the minimal influence of Maillard reaction on proteins in the acidic solutions (Ajandouz et al., 2010), and its decreasing net charges near the IEP. As shown in Fig. 4(a), the insoluble white aggregates firstly decreased and subsequently increased in each vertical column with the increase of pH value. The smaller and more uniform apparent morphology were observed by naked eye in the gel particles incubated at the environment pH of 4.2 and that would be the optimized pH value for further analysis.

3.8. Morphology observation and dimensional determination of SPI-SSPS gel particles

As displayed in Fig. 4(b), the brighter grey hydrophobic cores of SPI were surrounded by dark hydrophilic SSPS, where the soybean protein, soybean polysaccharide and protein-polysaccharide conjugate were revealed bright white particles or the dark irregular part around the gel particles, because of the negative staining of uranium acetate, as less or no dye was deposited on the surface of dense core (gel particles). According to the core–shell theory, stable gel particles would be built with the hydrophobic forces and disulfide linkage between the each molecules in the acidic solutions below the IEP and presented as a protein-core and polysaccharides-shell (Wagoner et al., 2016).

The approximately spherical gel particles were further presented by using TEM (Fig. 4(b)) and SEM (Fig. 4(c)) observations, meanwhile the size discrepancies were also analysed based on the images. Generally, the particle sizes of the native and pH 1.5 shifting SPI were in the range of 100–150 nm, while those of pH 2.5 and 3.5 were less than 100 nm according to the images. Moreover, the Z-average of particle size was about 100–250 nm and the SPI-SSPS gel particle prepared by native SPI was 223.13 ± 4.22 nm exactly in solution (Table 2). To obtain more information about interaction forces on the particle formation, the particle size distribution of low-pH shifting SPIs have also been compared. The size range of SPIs was about 300–500 nm, which linked to protein aggregation resulting from hydrophobic interaction, and further this force was regulated by glycosylation in SPI-SSPS gel particles. Since enhanced hydrophobicity via pH pre-treatment was confirmed in previous structural analysis, as well as aggregation and gelation of SPI were promoted via heat-induced process, a larger core with hydrophobic aggregation between SPI-SPI molecules would be established to the larger size of gel particle. However, except for pH 1.5 shifting group, the particle sizes of SPI-SPSS gels were decreased with the SPI treated pH values increasing in other pH shifting groups, which might be attributed to the reduction of hydrophobic aggregation. For the native SPI-SPSS gel particle, the increased size might attribute to the smaller glycosylated degree that could not prevent the protein aggregations.

3.9. Hydrophobicity promoted the colloidal solution stability of SPI-SSPS gel

The Zeta potential of each sub-micron gel particles in solution was determined (Table 2). According to Zeta potential analysis of Ding and Yao (2013), the soy polysaccharide was negatively charged while soy protein was positively charged in the pH range of 3.0–5.3. Therefore, each sample displayed as negative potential in solution suggested that the gel particle had a SSPS surface. It is generally believed that Zeta potential of colloids has a good correlation with the stability, and the greater the positive or negative magnitude, the more stable it is to resist secondary aggregation (Wagoner et al., 2016). The absolute value of Zeta potential increased with the increase of pH value in the sub-micron gel, which indicated a greater stability on the formation of solution system. An enhancing stability of the gel particles prepared by pH shifting SPIs was also shown comparing to the native. Due to the solution of pH 4.2 near the isoelectric point of SPI, the positive charges of protein would be electrostatic shielded by the SSPS molecules which were cross-linked with SPIs with a large amount of negative charges. The formation of larger aggregates was prevented through the intermolecular electrostatic repulsion of polysaccharides and maintained the stability of sub-micron gel particles.

3.10. Mechanism of SPI-SSPS gel particles formation with self-assembly

The self-assembly of nano-gel particles was realized through the intermolecular non-covalent bonds, specifically, interactions between molecules or molecules and solvents to achieve the micellization of amphiphilic polymers. The hydrophobic proteins from amphiphilic conjugates spontaneously aggregate and nucleate driven by entropy, and meanwhile, the water-soluble blocks surround the hydrophobic core to form shells in aqueous solution. These natural amphiphilic polymers are usually obtained by hydrophilic/hydrophobic modification of proteins. Therefore, here we built SPI-SSPS conjugates by low-pH shifting and glycosylated treatments of SPI for preparing gel particles.

The formation of sub-micron SPI-SSPS gel particles mainly covered three stages: the low-pH shifting modification as well as glycosylation of SPI and the construction of gel particles from SPI-SSPS conjugates (Fig. 4(d)). In fact, the above design came from the demand of nanomaterial interaction forces for self-assembly. The pH shifting treatment is a process by means of exposing the substance to extreme pH incubation followed by neutralization (Jiang et al., 2012), and the globulin with a kinetic intermediate for reversible denaturation would be produced under mild denaturing conditions like extreme pH and high-pressure treatments and named the molten globule (MG) state (Hirose and Masaaki, 1993). Actually, the improved hydrophobicity, gelling property and solubility of SPI were proved after acidic or alkaline

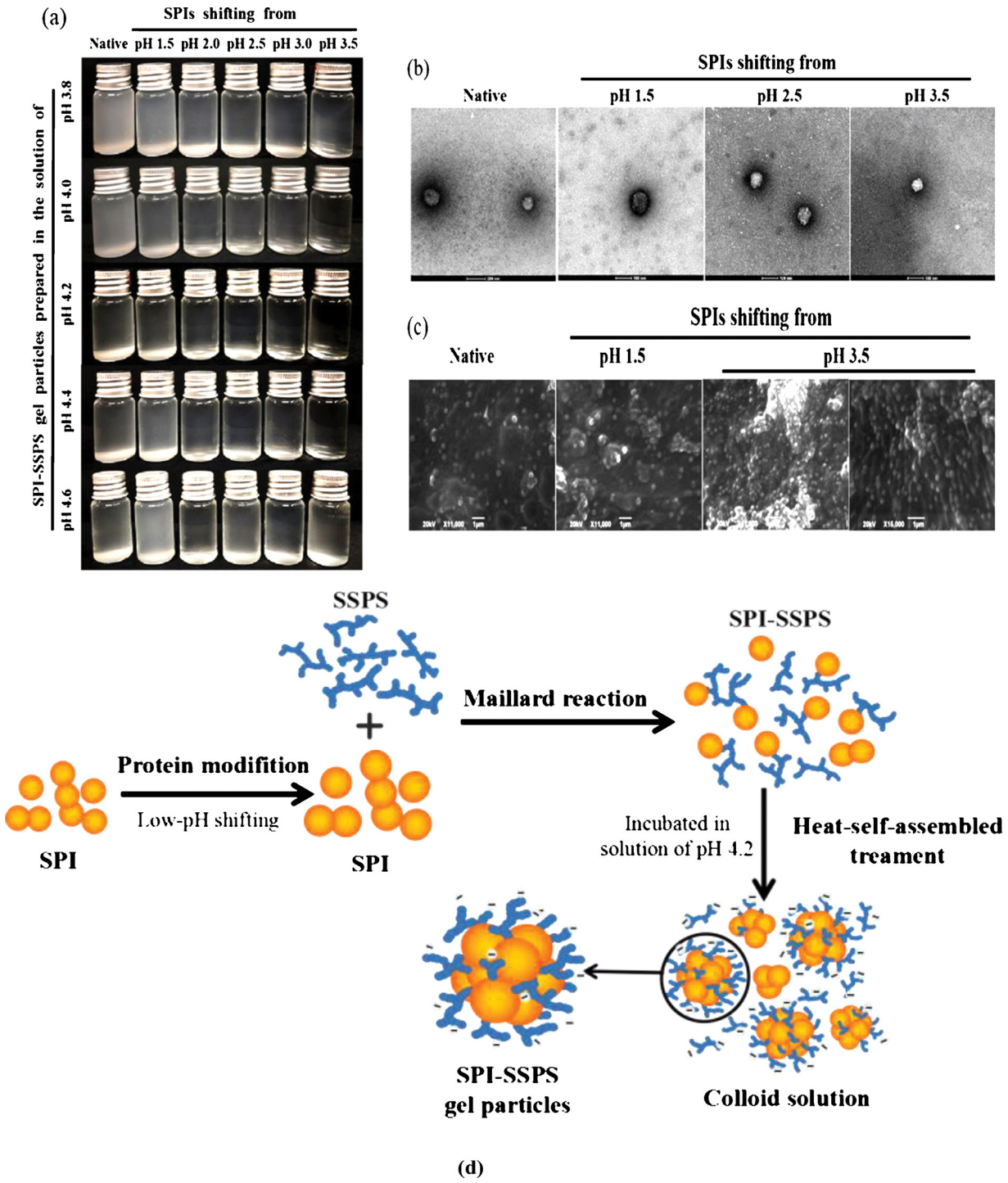

Fig. 4. Selection of incubated pH conditions and morphology observation. (a) The SPI-SSPS gel particles prepared in different pH solutions. (b) Gel particles prepared by the native SPI and SPIs shifting from pH 1.5, 2.5, and 3.5, respectively, via TEM. (c) Gel particles prepared by the native SPI (×11,000), the SPI shifting from pH 1.5 (×11,000), and 3.5 (×11,000, ×15,000), respectively, via SEM. (d) Schematic diagram of SPI-SSPS gel particles in design and build process.

treatment and suggested the further targeted and practical application. In the second step, the SPI-SSPS conjugates were created by Maillard reaction covalently attaching SPI onto SSPS skeletons. The water-soluble shell (SSPS) with negative charges would ensure the independence of particles and effectively prevented the adsorption of hydrophilic proteins when incubation in acidic solution, and that inhibited the over-aggregation even precipitation caused by simple hydrophobic interaction as well. Besides, the hydrophobic nucleus and the external environment were separated and presumably conducive to the embedding drugs to some extent.

Present studies ended in the observation of near spherical sub-micron gel particles and being stable in the acidic aqueous solution. While these results partly satisfied our initial assumptions—the direct effect of force regulation on gel formation and particle size. Simply, the formation of gel particles would be determined by the enhanced and controllable hydrophobic force of SPI and electostatic interaction triggered by SSPS. The more transparent colloidal solution was exhibited when SPI-SPSS gel was incubated in pH 4.2 solution (Fig. 4(a)), revealing the relative balance of hydrophobic interaction between proteins and electrostatic repulsion of polysaccharides. Moreover, greater particle

Table 2
Particle size distribution and Zeta potential analysis of SPI-SSPS gel particles.

Samples	Z-average(nm)		PdI		Zeta potential (mV)
	SPIs	SPI-SSPS particles	SPIs	SPI-SSPS particles	
Native	308.60 ± 11.52^{e}	223.13 ± 4.22^{b}	0.26 ± 0.02^{c}	0.28 ± 0.01^{b}	−1.79 ± 0.11^{a}
Shifting from pH 1.5	496.53 ± 13.95^{a}	256.20 ± 1.49^{a}	0.33 ± 0.00^{a}	0.24 ± 0.01^{c}	−2.80 ± 0.92^{a}
Shifting from pH 2.0	433.63 ± 5.97^{b}	189.43 ± 6.31^{c}	0.32 ± 0.01^{ab}	0.25 ± 0.01^{c}	−3.68 ± 0.18^{ab}
Shifting from pH 2.5	376.93 ± 10.30^{c}	146.80 ± 3.01^{d}	0.30 ± 0.00^{b}	0.28 ± 0.00^{b}	−5.26 ± 1.56^{bc}
Shifting from pH 3.0	350.20 ± 7.04^{d}	105.83 ± 2.12^{e}	0.31 ± 0.01^{ab}	0.29 ± 0.01^{b}	−7.43 ± 0.33^{c}
Shifting from pH 3.5	328.73 ± 4.29^{de}	95.08 ± 1.90^{f}	0.30 ± 0.01^{ab}	0.31 ± 0.01^{a}	−10.12 ± 0.30^{d}

Different lowercase letters indicate significant differences ($P < 0.05$) between each other in the same column.

size was observed in the SPI-SSPS gel by using the pH 1.5 shifting SPI than the native protein due to the hydrophobic aggregation of proteins, resulting from more exposures of hydrophobic groups or larger hydrophobic cavities; however, average gel particle sizes decreased with the increasing of pH shifting value of SPI, and the particle size reached 95.08 ± 1.90 nm by using the SPI shifting from pH 3.5. In addition, the extreme pH treatment also resulted in the increase of glycosylation degree, but in general, the hydrophobic force played a key role in the previous incubated condition (pH 4.2, 90 °C) for the SPI-SPSS gel formation.

The ideal model of delivery particle was a hydrophobic inner cavity formed by a layer of protein for loading drugs and maintaining near ball shape in details, while hydrophilic and negatively charged polysaccharide chains would ensure the colloid stability of single particle, but the globulins could built denser nucleus in the condition, which might have associations with the loading capacity of particle for hydrophobic compositions and particle size controlled by the hydrophobicity. The gel particle size would not be the bigger or smaller the better, but the approximate scale should be considered on account of specific applied environment. The average diameter of 7–9 μm of blood capillaries and/or 10–20 μm of somatic cells, although comparison would be inappropriate but intuitive, there might be unremarkable differences between the sub-micron and nano-meter scale particles to pass through tissues smoothly. Further evaluations of SPI-SSPS gel particles would focus on the drug-loadable capacity and environmental stability. Since the hydrophobic drugs would be effectively inserted into the hydrophobic cavity formed by amphoteric proteins and electrostatic forces would also be involved in the binding process, the original hypothesis about the balance between the hydrophobic protein and cross-linking of polysaccharide should be paid more attentions.

4. Conclusions

The changes of structure and physicochemical properties of low-pH shifting SPI were studied, and their applications on sub-micron gel formations were further discussed. Low-pH shifting could slightly alter the secondary structure of SPI, which increased the protein hydrophobicity and promoted the improvement of gelling property. Extreme pH treatment (pH 1.5) was not conducive to the gel formation, and the increased gel strength were displayed by using the SPIs shifting from pH 3.0 and 3.5. The glycosylation ability of SPI would be improved by low-pH shifting treatment and the SPI-SPSS conjugates could be used for preparing the biomaterial gel particles. Furthermore, the core–shell structure of sub-micron size could be formed and kept stability in the solution of pH 4.2 with the particle size range of 100–250 nm because of the appropriate balance between the hydrophobic protein and cross-linking of polysaccharide. Overall, extreme pH treatments would favour to the enhancement of hydrophobicity, and further would be beneficial to the formation of gel particles through self-assembly by means of the glycosylation and thermal induction. Hence, our results could provide a high-quality gel processing procedure for plant proteins.

Declaration of competing interests

The authors declare that they have no known competing financial interests or personal relationships that could have appeared to influence the work reported in this paper.

CRediT authorship contribution statement

Yufei Yang: Investigation, Methodology, Writing - original draft. **Shudong He:** Conceptualization, Methodology, Writing - review & editing, Supervision, Funding acquisition. **Yongkang Ye:** Validation, Resources, Funding acquisition. **Xiaodong Cao:** Validation, Resources, Funding acquisition. **Haiyan Liu:** Resources, Funding acquisition. **Zeyu Wu:** Validation, Resources. **Junyang Yue:** Validation, Resources. **Hanju Sun:** Data curation, Supervision, Project administration, Funding acquisition.

Acknowledgements

The authors are grateful for the financial support from the National Natural Science Foundation of China (No. 31701524), Chengdu Technological Innovation Research and Development Project, China (No. 2019-YF05-00965-SN), the Anhui Key Research and Development Program, China (No. 201904a06020030), 2019 CAST Outstanding Chinese and Foreign Youth Exchange Program and the Fundamental Research Funds for the Central Universities, China (No. JZ2019YYPY0295).

References

Ajandouz, E.H., Tchiakpe, L.S., Ore, F.D., Benajiba, A., Puigserver, A., 2010. Effects of pH on caramelization and Maillard reaction kinetics in fructos-lysine model systems. J. Food Sci. 66 (7), 926–931.
Bar-Zeev, M., Assaraf, Y.G., Livney, Y.D., 2016. β-casein nanovehicles for oral delivery of chemotherapeutic drug combinations overcoming P-glycoprotein-mediated multidrug resistance in human gastric cancer cells. Oncotarget 7 (17), 23322–23334.
Batista, A.P., Portugal, C.A.M., Sousa, I., Crespo, J.G., Raymundo, A., 2005. Accessing gelling ability of vegetable proteins using rheological and fluorescence techniques. Int. J. Biol. Macromol. 36 (3), 135–143.
Biswas, A., Bayer, I.S., Biris, A.S., Wang, T., Dervishi, E., Faupel, F., 2012. Advances in top–down and bottom–up surface nanofabrication: techniques, applications & future prospects. Adv. Colloid Interface Sci. 170 (1-2), 2–27.
Britto, D.D., Moura, M.R.D., Aouada, F.A., Pinola, F.G., Lundstedt, L.M., Assis, O.B.G., Mattoso, L.H.C., 2014. Entrapment characteristics of hydrosoluble vitamins loaded into chitosan and N, N, N-trimethyl chitosan nanoparticles. Macromol. Res. 22 (12), 1261–1267.
Buriti, F.C.A., dos Santos, K.M.O., Sombra, V.G., Maciel, J.S., Teixeira Sá, D.M.A., Salles, H.O., Oliveira, G., de Paula, R.C.M., Feitosa, J.P.A., Moreira, A.C.O.M., 2014. Characterisation of partially hydrolysed galactomannan from Caesalpinia pulcherrima seeds as a potential dietary fibre. Food Hydrocoll. 35 (3), 512–521.
Champagne, C.P., Fustier, P., 2007. Microencapsulation for the improved delivery of bioactive compounds into foods. Curr. Opin. Biotech. 18 (2), 184–190.
Chen, F.P., Ou, S., Tang, C.H., 2016. Core–shell soy protein-soy polysaccharide complex (nano)particles as carriers for improved stability and sustained-release of curcumin. J. Agric. Food Chem. 64 (24), 5053–5059.
Clark, A.H., Kavanagh, G.M., Ross-Murphy, S.B., 2001. Globular protein gelation—theory and experiment. Food Hydrocoll. 15 (4), 383–400.
Ding, X., Yao, P., 2013. Soy protein/soy polysaccharide complex nanogels: folic acid loading, protection, and controlled delivery. Langmuir 29 (27), 8636–8644.

Ellman, G.L., 1959. Tissue sulfhydryl groups. Arch. Biochem. Biophys. 82 (1), 70–77.
Fernandez-Avila, C., Arranz, E., Guri, A., Trujillo, A.J., Corredig, M., 2016. Vegetable protein isolate-stabilized emulsions for enhanced delivery of conjugated linoleic acid in Caco-2 cells. Food Hydrocoll. 55, 144–154.
Gu, X., Campbell, L.J., Euston, S.R., 2009. Influence of sugars on the characteristics of glucono-δ-lactone-induced soy protein isolate gels. Food Hydrocoll. 23 (2), 314–326.
Hirose, Masaaki, 1993. Molten globule state of food proteins. Trends Food Sci. Tech. 4 (2), 48–51.
Huang, Y., Hua, Y., Qiu, A., 2006. Soybean protein aggregation induced by lipoxygenase catalyzed linoleic acid oxidation. Food Res. Int. 39 (2), 240–249.
Hwang, D.C., Damodaran, S., 2015. Metal-chelating properties and biodegradability of an ethylenediaminetetraacetic acid dianhydride modified soy protein hydrogel. J. Appl. Polym. Sci. 64 (5), 891–901.
Jiang, J., Xiong, Y.L., 2013. Extreme pH treatments enhance the structure-reinforcement role of soy protein isolate and its emulsions in pork myofibrillar protein gels in the presence of microbial transglutaminase. Meat Sci. 93 (3), 469–476.
Jiang, J., Chen, J., Xiong, Y.L., 2009. Structural and emulsifying properties of soy protein isolate subjected to acid and alkaline pH-shifting processes. J. Agric. Food Chem. 57 (16), 7576–7583.
Jiang, J., Xiong, Y.L., Chen, J., 2011. Role of β-conglycinin and glycinin subunits in the pH-shifting-induced structural and physicochemical changes of soy protein isolate. J. Food Sci. 76 (2), C293–C302.
Jiang, J., Xiong, Y.L., Newman, M.C., Rentfrow, G.K., 2012. Structure-modifying alkaline and acidic pH-shifting processes promote film formation of soy proteins. Food Chem. 132 (4), 1944–1950.
Kato, A., Tsutsui, N., Matsudomi, N., Kobayashi, K., Nakai, S., 1981. Effects of partial denaturation on surface properties of ovalbumin and lysozyme. Agric. Biol. Chem. 45 (12), 2755–2760.
Kristinsson, H.G., Hultin, H.O., 2004. Changes in trout hemoglobin conformations and solubility after exposure to acid and alkali pH. J. Agric. Food Chem. 52 (11), 3633–3643.
Lammel, A.S., Hu, X., Park, S.H., Kaplan, D.L., Scheibel, T.R., 2010. Controlling silk fibroin particle features for drug delivery. Biomaterials 31 (16), 4583–4591.
Li, J., Yao, P., 2009. Self-assembly of ibuprofen and bovine serum albumin-dextran conjugates leading to effective loading of the drug. Langmuir 25 (11), 6385–6391.
Li, J., Yu, S., Yao, P., Jiang, M., 2008. Lysozyme-dextran core–shell nanogels prepared via a green process. Langmuir 24 (7), 3486–3492.
Liu, R., Zhao, S., Xiong, S., Xie, B., Qin, L., 2008. Role of secondary structures in the gelation of porcine myosin at different pH values. Meat Sci. 80 (3), 632–639.
Liu, Q., Geng, R., Zhao, J., Chen, Q., Kong, B., 2015. Structural and gel textural properties of soy protein isolate when subjected to extreme acid pH-shifting and mild heating processes. J. Agric. Food Chem. 63 (19), 4853–4861.
Liu, T.X., Zhao, M., 2010. Physical and chemical modification of SPI as a potential means to enhance small peptide contents and antioxidant activity found in hydrolysates. Innov. Food Sci. Emerg. 11 (4), 677–683.
Manassero, C.A., Vaudagna, S.R., Añón, M.C., Speroni, F., 2015. High hydrostatic pressure improves protein solubility and dispersion stability of mineral-added soybean protein isolate. Food Hydrocoll. 43, 629–635.
Molina, E., Ledward, D.A., 2003. Effects of combined high-pressure and heat treatment on the textural properties of soya gels. Food Chem. 80 (3), 367–370.
Nasrollahzadeh, F., Varidi, M., Koocheki, A., Hadizadeh, F., 2017. Effect of microwave and conventional heating on structural, functional and antioxidant properties of bovine serum albumin-maltodextrin conjugates through Maillard reaction. Food Res. Int. 100 (Pt 2), 289–297.
Nooshkam, M., Madadlou, A., 2016. Microwave-assisted isomerisation of lactose to lactulose and Maillard conjugation of lactulose and lactose with whey proteins and peptides. Food Chem. 200, 1–9.
Paulson, A.T., Tung, M.A., 1989. Thermally induced gelation of succinylated canola protein isolate. J. Agric. Food Chem. 37 (2), 319–326.
Pawar, H.A., Lalitha, K.G., 2014. Isolation, purification and characterization of galactomannans as an excipient from Senna tora seeds. Int. J. Biol. Macromol. 65 (2), 167–175.
Penas, E., Prestamo, G., Gomez, R., 2004. High pressure and the enzymatic hydrolysis of soybean whey proteins. Food Chem. 85 (4), 641–648.
Prado, B.M., Kim, S., Özen, B.F., Mauer, L.J., 2005. Differentiation of carbohydrate gums and mixtures using Fourier transform infrared spectroscopy and chemometrics. Food Chem. 53 (8), 2823–2829.
Przybyla, D.E., Chmielewski, J., 2010. Higher-order assembly of collagen peptides into nano- and microscale materials. Biochemistry 49 (21), 4411–4419.
Ptitsyn, O.B., Pain, R.H., Semisotnov, G.V., Zerovnik, E., Razgulyaev, O.I., 1990. Evidence for a molten globule state as a general intermediate in protein folding. FEBS Lett. 262 (1), 20–24.
Puppo, C., Chapleau, N., Speroni, F., de Lamballerie-Anton, M., Michel, F., Añón, C., Anton, M., 2004. Physicochemical modifications of high-pressure-treated soybean protein isolates. J. Agric. Food Chem. 52 (6), 1564–1571.
Rabanel, J.M., Aoun, V., Elkin, I., Mokhtar, M., Hildgen, P., 2012. Drug-loaded nanocarriers: passive targeting and crossing of biological barriers. Curr. Med. Chem. 19 (19), 3070–3102.
Renkema, J.M.S., Gruppen, H., van Vliet, T., 2002. Influence of pH and ionic strength on heat-induced formation and rheological properties of soy protein gels in relation to denaturation and their protein compositions. J. Agric. Food Chem. 50 (21), 6064–6071.
Sáizabajo, M.J., Gonzálezferrero, C., Morenoruiz, A., Romohualde, A., Gonzáleznavarro, C.J., 2013. Thermal protection of β-carotene in re-assembled casein micelles during different processing technologies applied in food industry. Food Chem. 138 (2–3), 1581–1587.
Speroni, F., Beaumal, V., Lamballerie, M.D., Anton, M., Añón, M.C., Puppo, M.C., 2009. Gelation of soybean proteins induced by sequential high-pressure and thermal treatments. Food Hydrocoll. 23 (5), 1433–1442.
Sun, C., Du, K., Chen, F., Bhattarai, N., Veiseh, O., Kievit, F., Stephen, Z., Lee, D., Ellenbogen, R.G., Ratner, B., 2010. PEG-mediated synthesis of highly dispersive multifunctional superparamagnetic nanoparticles: their physicochemical properties and function in vivo. ACS Nano 4 (4), 2402–2410.
Sun, Q., He, J., Yang, H., Li, S., Zhao, L., Li, H., 2017. Analysis of binding properties and interaction of thiabendazole and its metabolite with human serum albumin via multiple spectroscopic methods. Food Chem. 233, 190–196.
Tu, T., Rousseau, D., 2013. Stabilization of acidic soy protein-based dispersions and emulsions by soy soluble polysaccharides. Food Hydrocoll. 30 (1), 382–392.
Wagoner, T., Vardhanabhuti, B., Foegeding, E.A., 2016. Designing whey protein-polysaccharide particles for colloidal stability. Annu. Rev. Food. Sci. Technol. 7 (1), 93–116.
Wang, X., Yucel, T., Lu, Q., Hu, X., Kaplan, D.L., 2010. Silk nanospheres and microspheres from silk/pva blend films for drug delivery. Biomaterials 31 (6), 1025–1035.
Wang, Q., Sun, Q., Ma, X., Rao, Z., Li, H., 2015. Probing the binding interaction of human serum albumin with three bioactive constituents of Eriobotrta japonica leaves: spectroscopic and molecular modeling approaches. J. Photochem. Photobiol. B 148, 268–276.
Wang, L., Wu, M., Liu, H.-M., 2017. Emulsifying and physicochemical properties of soy hull hemicelluloses-soy protein isolate conjugates. Carbohyd. Polym. 163, 181–190.
Zhu, K., Ye, T., Liu, J., Peng, Z., Xu, S., Lei, J., Deng, H., Li, B., 2013. Nanogels fabricated by lysozyme and sodium carboxymethyl cellulose for 5-fluorouracil controlled release. Int. J. Pharm 441 (1-2), 721–727.